Advanced Review

Structural colors: from natural to artificial systems

Yulan Fu,[1] Cary A. Tippets,[2] Eugenii U. Donev[3] and Rene Lopez[1]*

Structural coloration has attracted great interest from scientists and engineers in recent years, owing to fascination with various brilliant examples displayed in nature as well as to promising applications of bio-inspired functional photonic structures and materials. Much research has been done to reveal and emulate the physical mechanisms that underlie the structural colors found in nature. In this article, we review the fundamental physics of many natural structural colors displayed by living organisms as well as their bio-inspired artificial counterparts, with emphasis on their connections, tunability strategies, and proposed applications, which aim to maximize the technological benefits one could derive from these photonic nanostructures. © 2016 Wiley Periodicals, Inc.

How to cite this article:
WIREs Nanomed Nanobiotechnol 2016. doi: 10.1002/wnan.1396

INTRODUCTION

Humans perceive the world in a colorful way because of the selective spectral sensitivities of the light receptors in our eyes' retinas. Objects presenting different light-spectrum distributions appear as possessing distinct colors. Several mechanisms for generating colors in materials are known, including preferential absorption, emission, birefringence, and photochromism. For a non-luminous object, we see a specific color if the object strongly reflects only a particular range of visible wavelengths. This can happen in two ways. On the one hand, the object absorbs part of the light spectrum due to interactions between the illuminating photons and electrons in the material, which is the general coloration mechanism of pigments, dyes, and metals. For example, the chlorophyll pigment found in many bacteria, algae, and plants absorbs most of the red and blue light from the sun and reflects green light, thus causing most vegetation to look green. On the other hand, light can be strongly reflected and/or deflected from reaching the eye because of the interaction of light with the structure of an object, as is the case with so-called structural colors. A familiar example of structural color is the atmospheric rainbow, which is caused by reflection, refraction, and dispersion of light in water droplets resulting in a spectrum of colors appearing in the sky.

There is a rich variety of structural colors in biology, such as the brilliant blue of the wings of *Morpho* butterflies, the iridescent colors of some beetles, and the vibrant metallic blue of the *Pollia* fruit.[1–3] Many efforts have been undertaken in the past decade or so to both reveal the origins of biological structural colors as well as replicate them. Inspired by the natural creatures sporting these colors, researchers have achieved substantial progress in developing functional photonic materials with vivid structural colors that could find applications in sensing technologies, security, light-emitting sources, paints, and other areas.[4–6]

Previous review articles have cataloged and explained in detail the structural colors found in nature.[7–9] In addition, other recent works have reviewed artificial structural coloration.[10–16] In this article, we focus on the connection between these two fields and explore the bridge between natural structural colors and the artificial structural colors they have inspired. The article is organized as

*Correspondence to: rln@physics.unc.edu

[1]Department of Physics and Astronomy, University of North Carolina at Chapel Hill, Chapel Hill, NC, USA

[2]Department of Applied Physical Sciences, University of North Carolina at Chapel Hill, Chapel Hill, NC, USA

[3]Department of Physics and Astronomy, The University of the South, Sewanee, TN, USA

Conflict of interest: The authors have declared no conflicts of interest for this article.

follows: Structural Color Physics section briefly reviews the basic physics behind structural coloration; Structural Colors in Nature section discusses various manifestations of structural color in biological species; and Inspired Structural Color section highlights the artificial structural colors generated by bio-inspired, artificially patterned, functional micro-/nanostructures.

STRUCTURAL COLOR PHYSICS

Thin-film Interference

Thin-film interference is perhaps the simplest source of structural color. It occurs when an incident light wave is reflected by each boundary of a thin film and the two reflected waves interfere with each other to form a new wave.[17] This mechanism can be seen if one considers a plane wave of light incident from a medium of refractive index n_1 on a thin film of refractive index n_2, as depicted in Figure 1(a). The incident and refracted angles are θ_1 and θ_2, respectively. The optical path difference (OPD) between the two reflected waves becomes:

$$\mathrm{OPD} = 2n_2 d\cos\theta_2.$$

If light is incident from a medium with a smaller refractive index onto a medium with a higher one, the reflected wave shifts its phase at the interface by an additional π radians. For a thin film in air, the condition for constructive interference of order m and wavelength λ then becomes:

$$2n_2 d\cos\theta_2 = \left(m-\frac{1}{2}\right)\lambda.$$

If the film is attached to a material with a higher refractive index, the constructive interference condition is:

$$2n_2 d\cos\theta_2 = m\lambda.$$

These simple relationships illustrate a dependence between the geometric structure of the film and the preferential wavelengths it reflects, giving rise to the perception of color when white light is incident upon the film. A soap bubble is a familiar manifestation of this mechanism and exemplifies the basis of more complicated structural coloration systems. The next stage of sophistication can be considered when multiple films are stacked on top of each other.

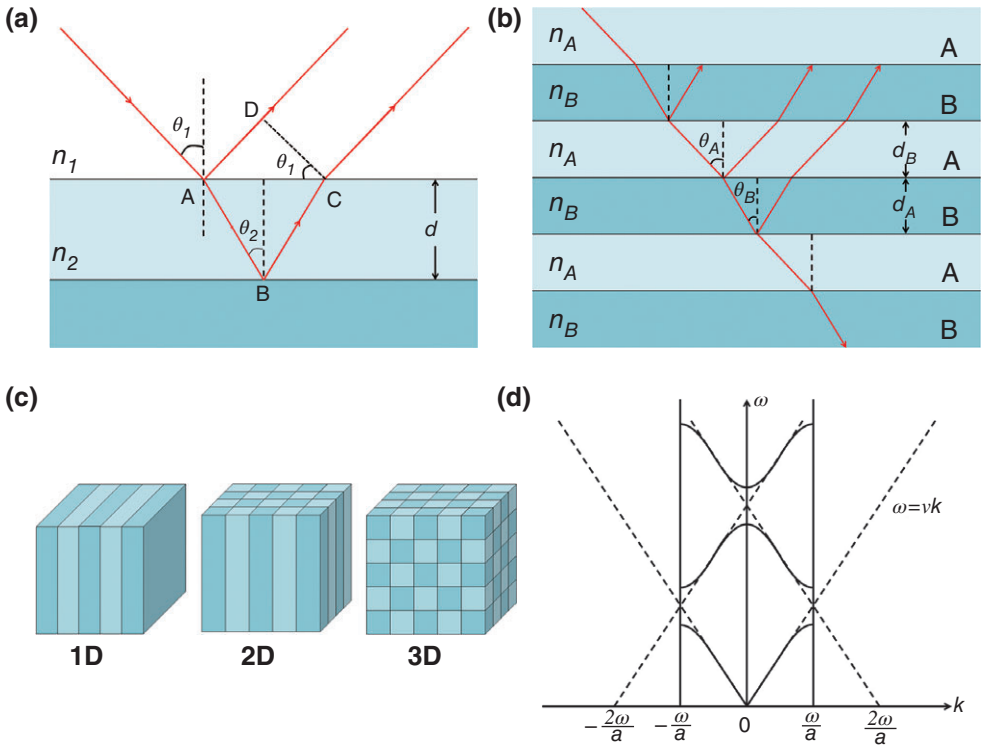

FIGURE 1 | (a) Two-beam interference in a single thin film. (b) Interference in multilayers (neglecting multiple reflections). (c) Schematics of 1D, 2D, and 3D photonic crystals. (d) Band dispersion diagram of a 1D photonic crystal.

Multilayer Interference

Multilayer photonic structures are composed of periodically stacked thin films with alternating high and low refractive indices, as shown in Figure 1(b). When a light wave is reflected from a multilayer consisting of different films A and B, with refractive indices n_A and n_B and thicknesses d_A and d_B, the condition for constructive interference is[17]:

$$2(n_A d_A \cos\theta_A + n_B d_B \cos\theta_B) = m\lambda.$$

This equation shows that, for incident sunlight, the apparent color of the multilayer reflector varies with the observation angle: as the angle of observation increases, the reflected color blueshifts toward shorter wavelengths. This effect occurs because the net OPD actually decreases even as the reflected waves travel longer distances through their respective layers, and thus constructive interference occurs for shorter wavelengths. The coloration tends to be more selective as the number of layers increases, resulting in very sharp reflection peaks with a strong angular dependence. This multilayer only has periodic index variation along one spatial dimension; one can intuitively expect similar physics could be observed in 2- and 3-dimensional structures.

Photonic Crystals

Photonic crystals (Figure 1(c)) are ordered nanostructures of two media with different refractive indices arranged in a spatially periodic fashion.[18,19] The multilayer periodic stacks discussed above can be considered a 1-dimensional (1D) photonic crystal. In higher dimensions, photonic crystals exhibit analogous behaviors to crystalline solids, providing a periodic potential for photons via the refractive index contrast as solids do for electrons through the lattice arrangement of ions. Figure 1(d) shows the band structure of a 1D photonic crystal, in which there is no electromagnetic field near $k \approx \pi/a$, where k is the wave vector and a is the crystal lattice constant. This region marks the bandgap for the electromagnetic wave. Light with a frequency within the bandgap cannot propagate in that direction, so this frequency of light experiences a high reflectivity and the photonic crystal appears a certain color. Two-dimensional (2D) photonic crystals are periodic in two directions, and their simplest realization consists of dielectric materials with air holes or dielectric pillars in air. In the plane of the 2D periodicity, light transmission and reflection are controlled by the photonic bandgaps mentioned above. Three-dimensional (3D) photonic crystals, have periodicities in all directions, and can confine and control light in three spatial dimensions via complete photonic bandgaps.

STRUCTURAL COLORS IN NATURE

Despite their complexity, photonic architectures are found in naturally formed structures such as opal stones and certainly in many biological materials. Their occurrence in a wide range of living species is indeed remarkable, as these animals, insects and plants manage to utilize the fundamental physical mechanisms described above to create variegated colors for their biological needs.

Morpho Butterflies

Among the structural colors displayed in nature, a truly spectacular example is the brilliant blue on the wings of the *Morpho* butterflies.[1,20] Figure 2 (a) shows a photograph of a *Morpho rhetenor*, which gives off a bright metallic blue color.[21] Under a low-power optical microscope, it can be observed that the back sides of the fore- and hind-wings are covered with tilted scales (Figure 2(b)). Closer optical inspection (Figure 2(c)) indicates that a single scale consists of seemingly parallel rows, while transmission electron microscopy (TEM) of a cross-section of a scale (Figure 2(d)) reveals that the rows themselves have complex nanostructures of ridges and lamellae.

The arrays of ridges and lamellae constitute three types of photonic crystal-like structures.[22–25] Firstly, thin films with air gaps and lamellae form a multilayer structure that gives rise to the blue color according to the interference condition. Secondly, a ridge is composed of a set of staggered lamella ('shelves') on the right and left sides that form two phase-shifted photonic crystals. When incident white light interacts with the two photonic crystals, the blue component scatters back to the source. Thirdly, the ridges of random height form a grating-like structure, yet the width, height, and lamella shape of each ridge contain some randomness that shifts the phases of reflected waves and cancels out the diffraction-grating effect.

The reflection, absorption, and transmittance of the wings of *M. rhetenor* are shown in Figure 2(e).[22] The reflection at wavelengths below 500 nm is high, with a peak reflectivity of 45% around 460 nm due to backward scattering. At other wavelengths, absorption in the pigments beneath the ridges also plays an important role: Removal of the complimentary color enhances the blue color and assures color saturation. The transmittance is quite weak below

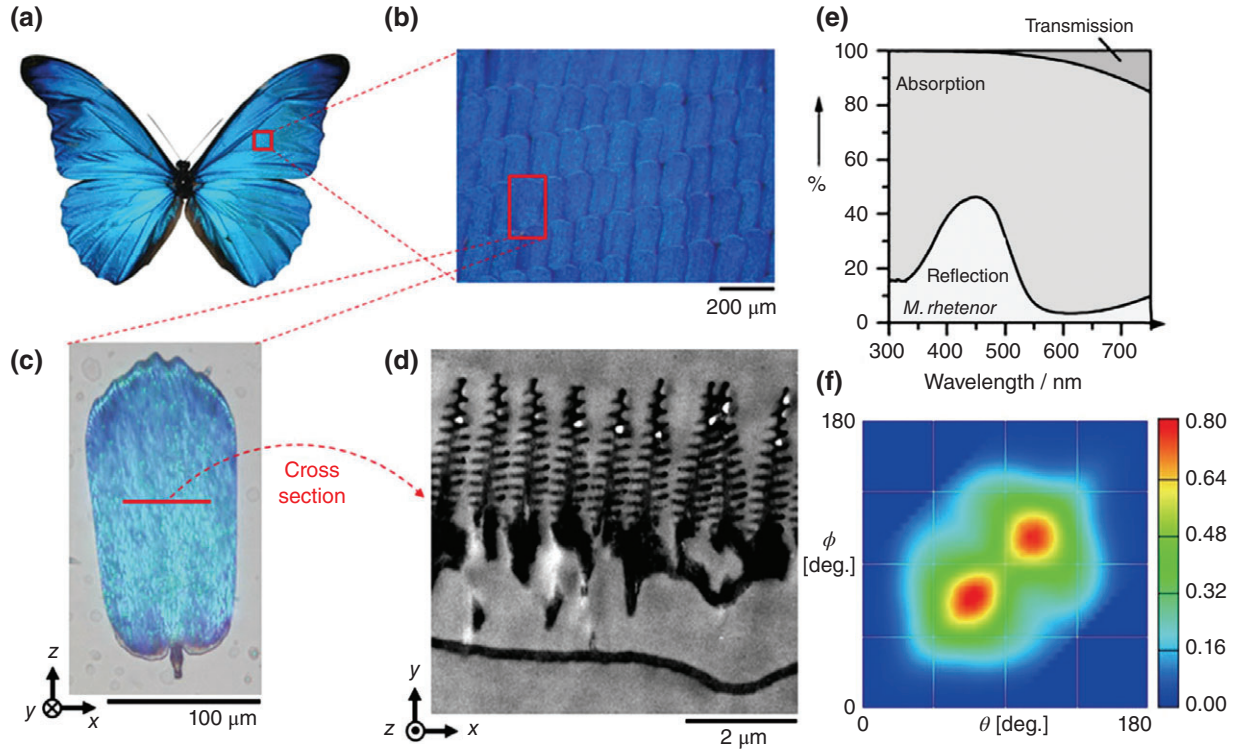

FIGURE 2 | (a) Photograph of a *Morpho rhetenor* butterfly.[21] (b) and (c) Scales of a *M. rhetenor* under microscope at low and high magnification, respectively. (d) TEM image of the ultrastructure on the *M. rhetenor* wing. (e) Reflection and absorption of the *M. rhetenor* wing. (f) Reflectance of a male *M. rhetenor* wing sample over the entire plane of incident (θ) and reflection (ϕ) angles.

500 nm and increases slightly toward the near-infrared region. Figure 2(f) shows the experimentally measured reflectance of a male *M. rhetenor* wing sample over the entire planar incident and reflection angular space, producing a high-intensity two-lobe θ-ϕ angular signature at peak reflectance that cannot be obtained by diffraction or multilayer interference alone.[26]

Three explanations have been proposed for the biological role of the blue coloration of the male of this species: (1) that the shimmering blue wings of the courting male attract a resting female; (2) that predatory birds may become disoriented by the 'blinking flash' of blue; (3) or that the blue color signals a territorial claim against other males, since a piece of blue metallic paper has been shown to attract female *Morpho* butterflies.[17]

Beetles

There are many types of beetles that reflect bright iridescent colors, which appear to change with the angle(s) of view and/or illumination. The mechanisms responsible for these colors can be classified in three groups: multilayer reflectors, 3D photonic crystals, and diffraction gratings. Various types of 3D photonic crystal structures have been found in the scales of beetles. For example, the photonic crystals found in the scales of *Pachyrrhynchus* and *Metapocyrtus* have a close-packed hexagonal arrangement analogous to opal, while the photonic crystal of *Lamprocyphus* has a diamond-based lattice.[27–29] A third kind of structural colors in beetles is caused by grating structures made of parallel ridges or slits, such as in *Serica sericea*, which diffract white light into its constituent wavelengths[30] to create rainbow-like reflectance.

Multilayer reflectors are perhaps the most common and best understood iridescence mechanism in beetles. Figure 3(a) shows a photograph images of this kind of natural reflector taken on a buprestid beetle, *Euchroma gigantean*.[31] Their hardened wing covers (elytra) have multilayer structures consisting of dark melanin layers and clear chitin layers (Figure 3(b) and (c)). The uppermost clear layer has a thickness of 0.2–0.4 μm, beneath which are dark layers of 0.09 μm thickness for the copper brown region of the elytra. The color reflected by a multilayer structure depends on the refractive index of the component layers and their periodicity. According to the multilayer interference condition given above, the

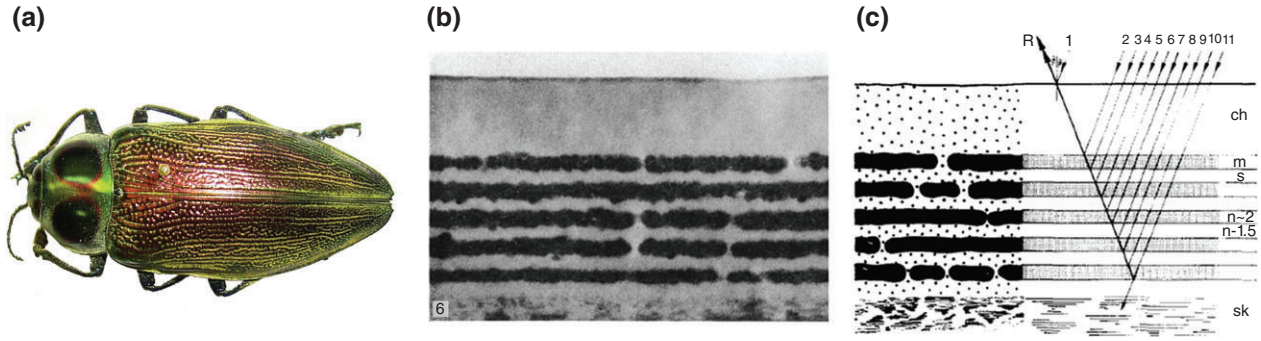

FIGURE 3 | (a) Photograph of *Euchroma gigantean* (https://en.wikipedia.org/wiki/Euchroma_gigantea). (b) TEM image of the elytra of E. gigantean (50,000×).[31] (c) Schematic of interference in the multilayer structures of the elytra of *E. gigantean*.

first-order wavelength of peak reflection at normal incidence equals $2(n_A d_A + n_B d_B)$, which shows that layers with a greater optical thickness (nd) reflect longer wavelengths than thinner layers. On the buprestid beetle, the reflector thickness varies between body regions, so colors of different hues may be reflected.

From an optics viewpoint, *Chrysina resplendens* is one of the most interesting beetle species owing to its brilliant metallic golden color.[32] These beetles have been found to reflect circularly polarized light from incident unpolarized sunlight.[33] Their elytra consist of two helicoidal layers sandwiching a layer of unidirectional molecular architecture.[34] The two helicoidal layers twist in opposite directions and produce the wideband reflection with specific circular polarizations. The sandwiched layer forms an excellent $\lambda/2$ retardation plate around 590 nm. When unpolarized light is incident normally to the material, the light with left-circular polarization is completely reflected, while that with right circular polarization penetrates without any loss. The $\lambda/2$ retardation plate changes right-circular light to left-circular light when transmitted. The converted left-circular light is then selectively reflected in the second cholesteric layer and the reflected light becomes left-circular. The $\lambda/2$ retardation plate again changes the left-circular light to right-circular light, which penetrates the first layer without loss and emerges out. Thus both left- and right-circular light are effectively reflected.

Peacock

The peacock feather demonstrates another excellent example of biological structural colors. The male peacock is one of the most beautiful birds: it has brilliant, iridescent, diversified colors, and intricate, colorful eye patterns. In Figure 4(a), one can see that the peacock tail feather has a central stem with an array of barbs on each side. Scanning electron microscope (SEM) images show the barb has lots of barbules.[35] A barbule consists of a medullar core of ~3 μm in diameter enclosed by a cortex layer; the cortex layers of differently colored barbules contain 2D photonic-crystal structures made up of melanin rods connected by keratin.[36] High-magnification TEM imaging clearly shows the lattice structure of the particles in a blue feather. The diameter of a particle is estimated at 130 and 140 nm for blue and yellow feathers, respectively, under the assumption that the particles are close-packed parallel to the surface. Blue and yellow feathers have 8–12 and 3–6 regular layers with layer intervals of 150 and 190 nm, respectively.[35] Below the lattice structure, the particles are randomly distributed. In contrast to the transverse cross-section, the particles have an elongated shape, up to several microns, in the longitudinal cross-section, and are rather randomly distributed.

To explore the origin of coloration in peacock feathers, the photonic band structure of an infinite 2D photonic crystal was calculated by a plane-wave expansion method, whereby a partial bandgap was found along the normal to the cortex surface for two polarization directions and at frequencies corresponding to observed strong reflections.[36,37] The simulation further reveals that the coloration is controlled by the lattice constant and number of periods in the photonic-crystal structure. Varying the lattice constant produces a variety of colors, while reducing of the number of periods brings out additional colors, causing mixed coloration.

Other Birds

Many other birds, such as hummingbirds and kingfishers (Figure 4(b)), have bright colors caused by nanostructures in their feathers. In China, the blue feathers of the kingfisher were traditionally used to decorate jewelry, and their color has not faded after hundreds of years. The colors of bird feathers can

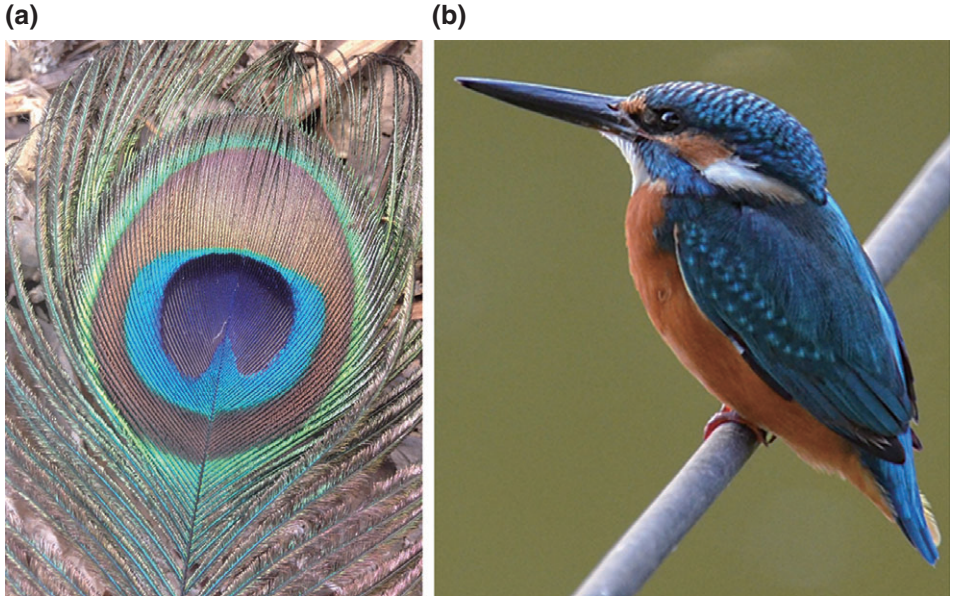

FIGURE 4 | (a) Photograph of a peacock tail feather. (https://en.wikipedia.org/wiki/Peafowl) (b) Photograph of a common kingfisher. (https://en.wikipedia.org/wiki/Common_kingfisher)

also be categorized as iridescent colors, that is, changing in appearance with the angle(s) of observation and/or illumination, and non-iridescent colors, which remain more or less visually constant regardless of the angle of observation.[38]

Iridescent structural colors in avian species are normally due to barbules composed of well-ordered melanin granules. The granules, arranged in a regular structure, play an important role in displaying structural colors, while absorption of the unnecessary complementary colors further enhances the vividness of the display. The hummingbird has iridescent green and blue colors in its head and breast, respectively.[39] Its iridescence is caused by interference effects in a stack of three films whose total optical thickness is one-half of the peak wavelength. The films consist of elliptical platelets of air bubbles encased in a matrix of refractive index of ~2. The different hummingbird colors are produced by a combination of effects: The platelet thickness decreases moderately across the spectrum from red through green to blue, and the air content increases simultaneously.

Non-iridescence was treated as arising from incoherent light scattering, such as Rayleigh scattering and Tyndall scattering. However, Prum et al.[40] studied the periodicity of the medullary keratin in the barbs. They performed a 2D discrete Fourier analysis of the spatial variation in refractive index of the spongy medullary keratin from four different colors of structurally colored feather barbs from three species of birds: *Agapornis roseicollis*, *Melopsittacus undulatus*, and *Poephila guttata*. The results indicate that the spongy medullary keratin is a nanostructured tissue that functions as an array of coherent scatterers. The nanostructure of the medullary keratin is nearly uniform in all directions, thus explaining the absence of iridescence. The largest Fourier components of the spatial variation of refractive index in the tissue are of the appropriate size to produce the observed colors by constructive interference alone. In the cyan and blue barbs of the common kingfisher, *Alcedo atthis,* there are spongy nanostructures with slightly different dimensions, causing different reflectance spectra.[41] In addition, a broadband background reflection is contributed by the cortex of the shiny feathers, especially when the feathers are illuminated from oblique directions.

Tunable Structural Colors in Animals

It is generally interpreted that the ability of chameleons to change color is due to dispersion/aggregation of pigment-containing organelles within dermal pigment sacks. However, Teyssier et al.[42] found in the skin of panther chameleons (*Furcifer pardalis*) two superposed thick layers of structural coloration containing specialized cells (iridophores) with guanine crystals of different sizes. The reptiles' color-shifting ability (see Figure 5(a)) is due to active tuning of a lattice of guanine nanocrystals within a superficial

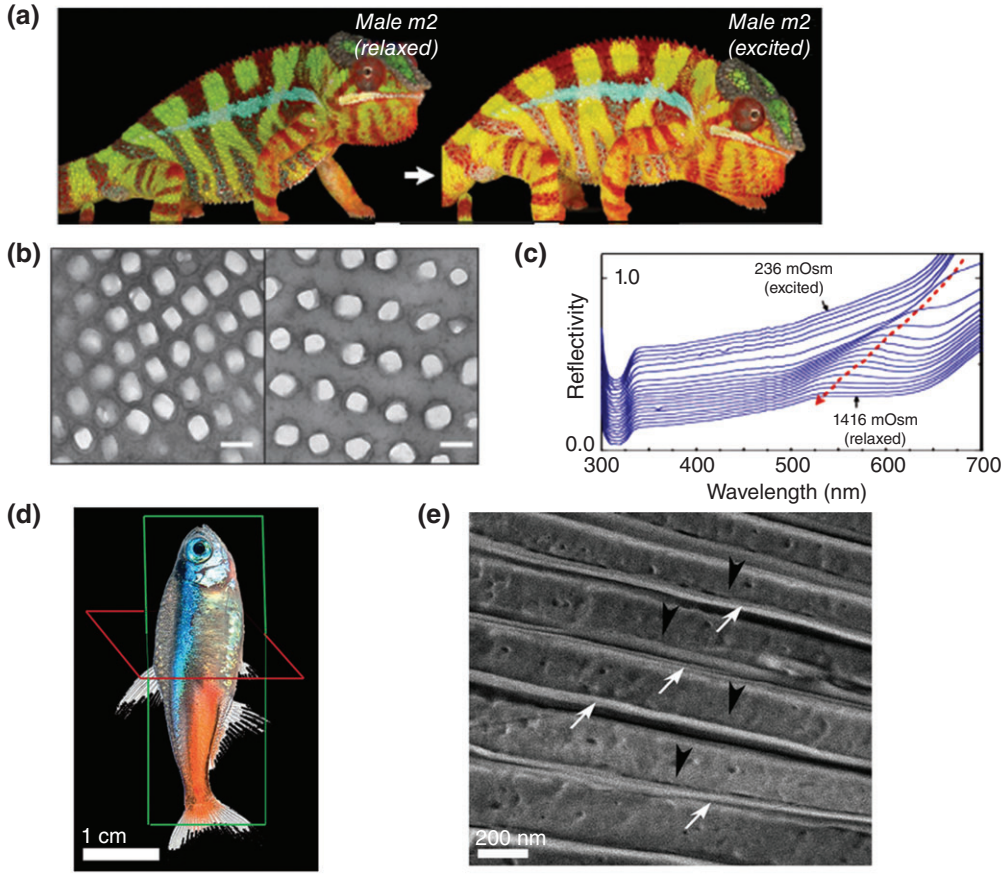

FIGURE 5 | (a) Reversible color change in the skin of a male panther chameleon from relaxed to excited state.[42] (b) TEM images of the lattice of guanine nanocrystals in S-iridophores from the same individual in a relaxed (left panel) and excited (excited panel) state. Scale bar, 200 nm. (c) Reflectivity of a chameleon skin sample with white skin osmolarity from 236 to 1416 mOsm. (d) Image of a light-adapted neon tetra fish with schematic outlines of the transversal (red) and longitudinal (green) sections of the stripe.[44] (e) Cryo-SEM images of a guanophore located in the lateral stripe of the neon tetra, in a section transversal to the stripe. White arrows, crystals; black arrow heads, cytoplasm.

thick layer of dermal iridophores. The deeper population of iridophores with larger crystals reflects a substantial proportion of sunlight, especially in the near-infrared range, which is likely advantageous for survival in hot dry environments.

The upper layer of iridophores is fully developed only in the skin of adult males, but reduced in the skin of females and juveniles. The iridophores in this layer contain small close-packed guanine crystals, with a diameter of 127.4 ± 17.8 nm (Figure 5 (b)), organized in a triangular lattice. The guanine crystals have a high refractive index of 1.83, while the cytoplasm has a low refractive index of 1.33, and together they form a photonic crystal structure. The TEM images of *F. pardalis* samples of blue or green skin (resting state; see left panel in Figure 5(a)) and images of yellow or white skin (excited state; see right panel in Figure 5(a)) of the same individuals showed that the distance among guanine crystals was on average 30% smaller in the resting than in the excited skin, while the crystal size in surface iridophores did not vary. Samples of excited skin (white/yellow) were subjected to hypertonic solutions to generate osmotic pressure likely to cause the guanine crystal lattice to shrink to its resting state. Figure 5 (c) shows a blue shift in the reflectivity of the iridophores due to this treatment. The color generated by a face-centered cubic lattice of close-packed guanine crystals was simulated for a range of lattice constants obtained from TEM images of various excited and unexcited male panther chameleon skin samples of different colors. The simulated reflected colors closely matched those observed *in vivo* and during the osmotic pressure experiments.

The chameleon's ability to change color is remarkable; nevertheless, color based on photonic crsytals is pervasive throughout the reptilian class. Saenko et al. found that the extensive variation in

color patterns within and among *Phelsuma* lizard species is generated by complex interactions between chromatophores containing yellow/red pteridine pigments and iridophores producing structural color by constructive interference of light with guanine nanocrystals.[43] These authors showed that the color patterns of *Phelsuma* always require precise co-localization of different sets of interacting pigmentary and structural elements. For example, yellow and red chromatophores are associated with iridophores with ordered and disordered nanocrystals, respectively.

Many other animals possess the ability to change colors in different environments. For instance, the neon tetra fish (Figure 5(d)) has the ability to change the color of its lateral stripe in response to a change in the light conditions, from blue-green in the light-adapted state to indigo in the dark-adapted state. A recent article[44] has shown that the reversible variations in crystal tilt within its individual crystal arrays are responsible for the light-induced color variations.

Different simulation methods have been utilized to explore the structural color of living creatures. In Table 1, we list some of these animals along with their type of color nanostructure and the optical simulation methods employed in the literature.

INSPIRED STRUCTURAL COLOR

The structural colors in nature illustrate paths toward producing artificial photonic structures that could find usage in security,[4] sensor,[5] display,[45] light-emitting sources,[6] and cosmetics[46] applications. The proposed applications of bio-inspired structural colors have thus far been primarily based on opal photonic crystals due to their ease of nanofabrication on large scales. In contrast to the rigid mathematics of the photonic crystal theory, many living systems achieve structural coloration by virtue of a masterful mixing of periodic with random structures to open up a range of optical responses and perceived colors. Replicas of the *Morpho* butterfly structure are a good example of bio-inspired structural colors. Various fabrication methods have been presented to reproduce the butterfly-like colors, and a recent sensor application has been demonstrated.[47] The fabricating methods have been improved over the past few years to combine ordered and disordered features and the butterfly replicas are now close to the actual butterfly in terms of not only color but angular response as well. Moreover, some absorption has also been employed judiciously to enhance the purity of the structural colors. As many living species display structural and also tunable colors, artificial color-changing photonic structures that can modify their optical behavior in response to external stimuli have been widely studied for applications in sensors and displays. The connection between the natural and the artificial counterparts is indeed strong and runs deep from the early days of the optical theory. Below we highlight some of the latest laboratory-made structures that seek to employ not only photonic crystal theory but also nature's insight to achieve quasi-periodic and tunable designs.

Butterfly-like Structures

The nanostructures on the scales of *Morpho* butterfly wings integrate three design principles leading to the wide-angle reflection: alternating lamellar layers, 'Christmas tree'-like shape, and offsets between neighboring ridges. Siddique et al.[24] studied the individual effects systematically by 2D finite element method electromagnetic simulations of nanostructures of the *Morpho sulkowskyi* butterfly, showing how the reflection spectrum can be controlled by the design of the nanostructures. Furthermore, the same authors fabricated the simulated structures by electron-beam lithography (EBL). The resulting samples mimicked all important optical features of the original *Morpho* butterfly scales and featured the intense blue iridescence with a wide angular range of reflection. However, the structures fabricated by EBL were not standing upright like the ridges on the

TABLE 1 | Simulation Methods Utilized to Explore Living Structural Color

	Structures	Simulation Methods
Morpho Butterfly	Photonic crystal-like structures	Finite difference time domain[21–23,25] Finite element method[24]
Peacock	2D photonic-crystal structures made up of melanin rods	Plane wave expansion[36,37]
Birds with non-iridescent feathers	Spongy medullary keratin	2D discrete Fourier analysis[40]
Chameleon	Face-centered cubic lattice of guanine crystals	Block-iterative frequency domain[42]

butterfly scales; instead they lay flat on the silicon substrate.

Huang et al.[48] replicated the exact structure of the butterfly by utilizing a butterfly wing as a biological template and coating it uniformly with Al_2O_3 (Figure 6(a)). This approach accurately reproduces the exact shape of the ultrastructure of the butterfly and the photonic bandgap can be tuned by infiltrating another material into the air spaces between the butterfly's lamellae and ridges. However, the need for destruction of the natural template limits the scale and applicability of any such device. A single *Morpho*-butterfly-scale quasi-structure (Figure 6(b)) was demonstrated by focused ion-beam (FIB) chemical vapor deposition (CVD).[49,50] The reflection spectra of the quasi-structure were very similar to those of the natural *Morpho* scales. This method was limited by the time and cost of fabricating each individual row of ultrastructures. Mukti et al.[51] combined chemical vapor deposition, ultraviolet (UV) nanolithography, and chemical etching methods to replicate the ultrastructures of the butterfly's wing scale out of a biomaterial multilayer on a substrate, covering a relatively large area with control of shapes, dimensions, and periodicity.

Inspired by the iridescent nanostructure and gradient surface chemistry of *Morpho* butterflies, Potyrailo et al.[47] fabricated 3D nanostructures that not only selectively detect individual closely related vapors in pristine dry-gas conditions, similar to the natural *Morpho* scales and conventional sensor arrays, but also quantify these vapors even in mixtures in the presence of a variable moisture background. The authors used EBL for the patterning of alternating layers of two types of positive-tone photoresist materials, poly(methyl methacrylate) (PMMA) and a copolymer of methyl methacrylate (MMA) and methacrylic acid (MAA), and then further selectively removed the MMA/MAA copolymer using a binary solvent to form intact PMMA lamellae. These individual multivariable sensors achieved quantification of small analyte concentrations in the presence of variable backgrounds, which is challenging for most sensor arrays.

Artificial Multilayers

To fabricate artificial multilayers with certain colors, the material indices and thicknesses need to be chosen according to the photonic bandgap theory. Typically, the multilayer photonic nanostructures are fabricated with two different materials with high and low refractive indices, and the types of materials vary from inorganic dielectric materials to organic polymers. Different coating methods can be utilized to fabricate multilayer reflectors, such as spin-coating and physical or chemical vapor deposition.

Choi et al.[5] realized porous, thin-film-based architectures with flexible compositions based on a sol–gel route to obtain all-mesoporous multilayer stacks. The layers were composed of alternating silica and titania slabs with pore sizes between roughly 3 and 10 nm, depending on the surfactant used as a template, and with porosities as high as 40%.

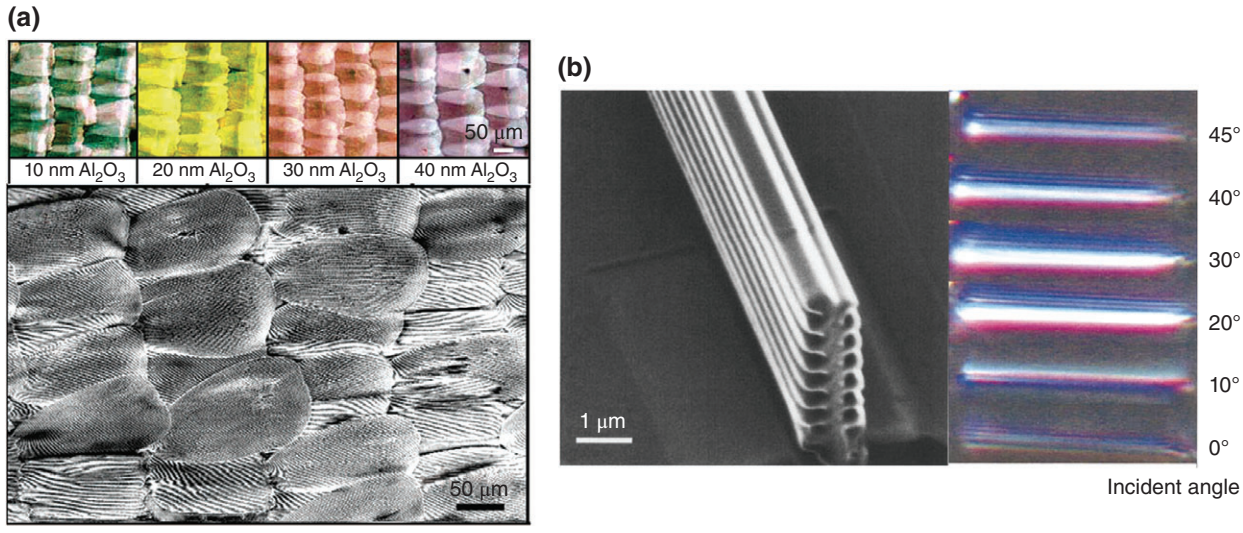

FIGURE 6 | (a) Optical microscope images of butterfly wing scales coated with different thickness of alumina and an SEM image of the alumina replicas of the butterfly wing scales after the butterfly template was completely removed.[48] (b) SIM images of *Morpho*-butterfly-scale quasi-structure fabricated by FIB-CVD and optical microscope images of the quasi-structure observed with a 5–45° incidence angle of white light.[50]

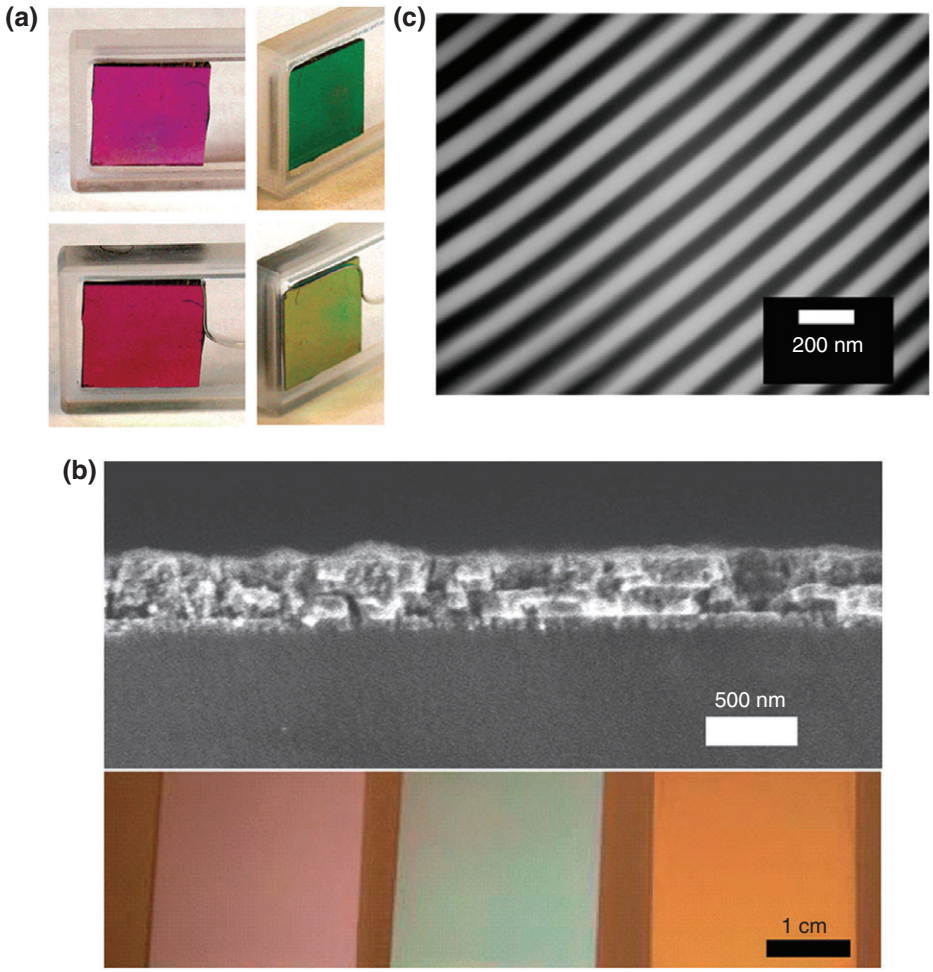

FIGURE 7 | (a) Four-layer mesoporous Bragg stack in air and in ethanol observed from different viewing angles.[5] (b) SEM image of five alternating regions of TiO_2 and SiO_2 nanoparticles and different structural colors of the films at normal incidence.[52] Different colors of the Bragg stacks were obtained by varying the number of deposited bilayers. (c) Bright-field TEM micrograph of cryomicrotomed PSb-PI block copolymer showing 1D periodic lamellar morphology.[53]

Investigation of the optical response of mesoporous multilayer stacks to a series of alcohols and alkanes (Figure 7(a)) revealed that their sensitivity and selectivity are highly dependent on the properties of the mesoporous metal oxide layers constituting the Bragg-reflector stack.

Wu and et al.[52] produced structural color in a titania/silica (TiO_2/SiO_2) nanoparticle system assembled by polyelectrolyte-assisted layer-by-layer deposition with subsequent calcination of the films to remove the polymer components. The resulting conformal, nanoporous thin-film coatings show the expected narrow-wavelength reflection bands that lead to analyte-sensitive structural color (Figure 7 (b)). The films also show favorable superhydrophilicity and self-cleaning properties.

Multilayer nanostructures can also be fabricated by self-assembly of organic dielectric materials. Yoon et al.[53] produced self-assembled polymeric distributed Bragg reflectors utilizing thin films of a lamellar-forming poly(styrene-b-isoprene) diblock copolymer with a high molecular weight, which can act as a photonic microcavity. The block copolymers phase-separate into periodic microdomains on the length scale of the blocks, driven by competition between the tendencies to reduce the interfacial free energy and to increase the conformational entropy of the constituting polymer chains. With an appropriate microdomain size that is large enough to interact with visible light, block copolymers can create periodic dielectric structures (Figure 7(c)) with a photonic stop band in the optical frequency range.

Colloidal Photonic Crystals

Brilliant structural color can be produced by packing colloidal nanoparticles.[16] A typical close-packed face-centered opal structure can be fabricated by depositing the colloidal nanoparticles in one of several different ways, among which the most straightforward method is sedimentation driven by gravitational forces.[54] During this process, the colloidal particles are allowed to settle down onto a substrate and pack into a hexagonal crystal lattice (Figure 8(a)). Faster deposition can be attained by enhanced gravitation via centrifugation, higher temperature, and/or external electric field.

To fabricate high-quality colloidal crystal films, a vertical suspension method was introduced by Jiang et al.[55] In this method, a substrate is immersed vertically into the colloidal suspension. During evaporation of the solvent, the colloidal particles begin to pin onto the substrate in the meniscus region, and then other colloidal particles move toward the pinned particles and assemble into an ordered structure driven by capillary forces (Figure 8(b)). However, the thickness of the film deposited with this method has a gradient because the suspension concentration increases as the solvent evaporates. To overcome this non-uniformity, Gu et al.[56] developed a 'lifting substrate' method, in which the substrate is lifted uniformly instead of sitting in the suspension (Figure 8(c)). With this method, colloidal film fabrication is much faster than the vertical deposition method, and the concentration of particles remains almost unchanged during the deposition, so that the thickness of the film is relatively uniform. Prevo et al.[57] developed a horizontal deposition method, in which time and material consumption can be decreased by steadily dragging a small volume of liquid confined in a meniscus between two plates (Figure 8(d)).

Angle Independence

Much of the bio-inspired structural colors have been realized by producing a bandgap, and hence the structural colors are usually iridescent. To produce non-iridescent colors, that is, independent of the observation and/or illumination angles, isotropic structures need to be employed. Amorphous photonic structures possess only short-range order but lack long-range periodicity. When the characteristic length scales are comparable to the wavelengths of visible light, amorphous photonic structures can produce

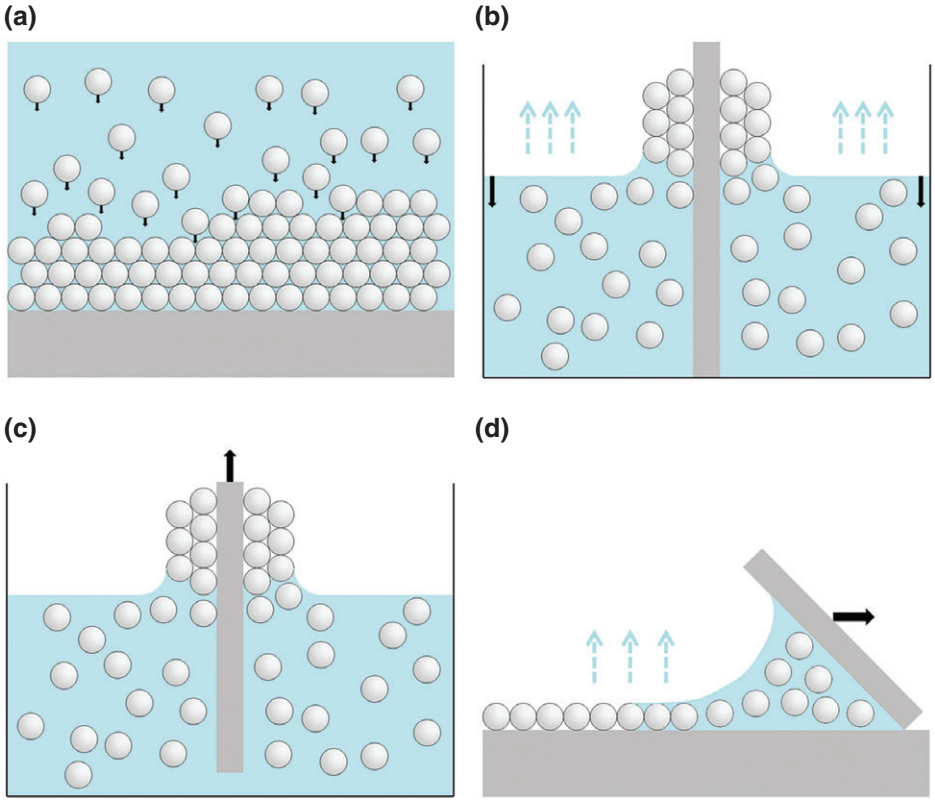

FIGURE 8 | Schematics of various methods for close-packed colloidal crystal formation: (a) natural sedimentation; (b) vertical deposition; (c) lifting substrate; (d) horizontal deposition.

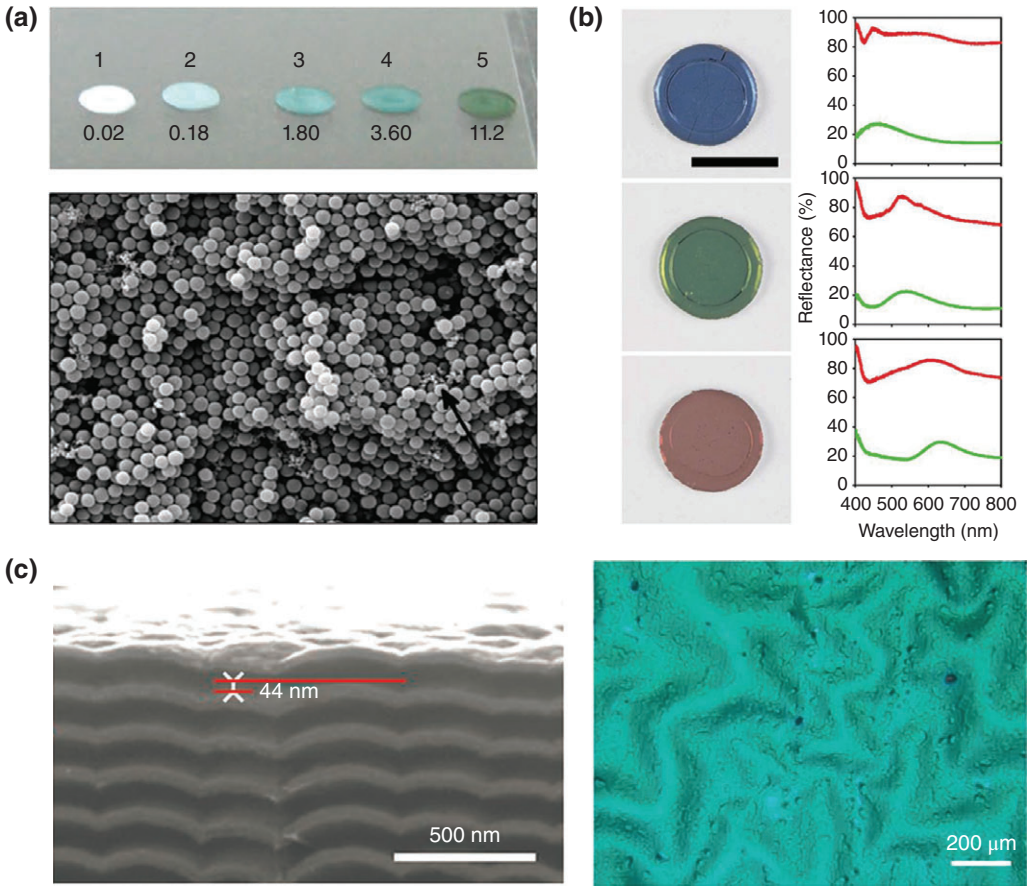

FIGURE 9 | (a) Side-view SEM image (bottom panel) of a film spin-coated 226 and 271 nm polystyrene spheres, and different structural colors (top panel) produced by different ratios of them.[58] (b) Images of the structural colors produced by different sizes of polystyrene spheres, and their reflectance spectra (with (red line) and without a water glue added).[59] Scale bars: 5 μm. (c) SEM and optical microscope images of a non-iridescent structure and its corresponding structural color.[60]

non-iridescent structural colors resulting from an isotropic photonic pseudogap, which is a partial energy (frequency) bandgap resulting from the disordered material. Forster and et al.[58] realized self-assembled isotropic films that display structural colors (Figure 9 (a)). The authors spin-cast a mixed suspension of two sizes of polystyrene spheres to ensures an isotropic structure. The transmission spectra of the isotropic film showed less angle independence than those of an anisotropic film self-assembled out of one-size spheres. They also added carbon-black paste to enhance wide-band absorption and avoid the sensitivity of the color to the film thickness, taking a lesson from animals that employ the absorption of complementary colors to 'purify' the structural colors.

Zhang and et al.[59] used cuttlefish ink as an additive to monodisperse polystyrene spheres with diameters between 200 and 300 nm to produce amorphous photonic structures with a high color visibility (Figure 9(b)). The cuttlefish ink consists of non-spherical melanin particles with an average size of about 110 nm, and its average absorption is about 99% in the visible range. The amorphous photonic structures with mixed nanoparticles showed different non-iridescent colors. When the relative proportion of cuttlefish ink particles was high, the resulting colors were darkish but non-iridescent. Conversely, when the relative proportion of cuttlefish ink was decreased, the colors tended to be bright and gradually became iridescent because of the ordering tendency of the polystyrene spheres.

To produce non-iridescent *Morpho* blue color, Chung et al.[60] spin-coated a random mixture of SiO_2 spheres with diameters between ~200 to 400 nm on a silicon wafer to form a loosely packed silica microsphere monolayer (Figure 9(c)). To ensure high color purity, the authors sputter-deposited chromium to provide a uniform dark background and reduce the back reflection of light transmitted through the

monolayer. Eight pairs of SiO_2 and TiO_2 layers were then sputter-deposited, and poly(dimethylsiloxane) (PDMS) was spin-coated on top to encase the entire sample. By controlling the layer thicknesses, different non-iridescent colors were obtained.

Tunable Structural Color

Based on the origin of the structural color, there are two essential approaches to achieve tunability: changing the refractive indices of the constituent materials and changing the lattice spacing of the photonic crystal. Ballato et al.[61] infiltrated a silicon opal with 1-methylnaphthalene (MN), which has a moderately high temperature coefficient of the refractive index (approximately -5×10^{-4}/K). When the temperature was increased, the refractive index of MN (nominally $n = 1.607$ at a wavelength of 656 nm and temperature of 25°C) decreased and the photonic bandgap of the opal structure shifted to shorter wavelengths, so the wavelength at the band edge moved out of the bandgap and its transmission increased. Relative percent changes in transmission of ~35% were observed over a temperature range of 12 K. This tunable structural color could be applied as a temperature sensor.

The molecular orientation of liquid crystals can be controlled by both temperature and electric field, so the structural colors of opals infiltrated with liquid crystals become tunable. Yoshino et al.[62] infiltrated SiO_2 opal structures with nematic or smectic liquid crystals. When the temperature was decreased from 75°C to 30°C, the refractive index of the liquid crystal was tuned by 0.012, and hence the bandgap position of the opal structure also shifted. Kubo et al.[63] added photochromic liquid-crystal AZO dyes into the infiltrated liquid crystal in the SiO_2 inverse opal, and realized photo-switchable photonic crystals. When the film was irradiated with UV light, *trans-cis* photoisomerization of the dye was induced, leading to the nematic-to-isotropic phase transition of the liquid crystal, and the emergence of a bandgap in the composite inverse opal.

To change the lattice spacing of colloidal crystals, Fudouzi et al.[64] infiltrated the void of an opaline lattice of polystyrene beads with a liquid prepolymer of PDMS, and then cured the PDMS. When 2-propanol was applied to the surface of the colloidal crystal, the crystal lattice of the opal structure was increased due to swelling of the PDMS network, and the color of the colloidal crystal was tuned from green to red. By infiltrating the swollen film with PDMS for a second time and curing it, the authors fixed the polystyrene opal as a non-close-packed array.[65] When the film was stretched mechanically in the horizontal direction, the lattice distance reduced in the vertical direction and the wavelength of the reflected light blueshifted; accordingly, the color of the PDMS sheet changed from red to green. When the mechanical strain on the sheet was released, the reflectance peak returned to its original spectral position, and the color changed back to red.

Yang et al.[66] developed an efficient and straightforward method for preparing a mechanochromic photonic gel by fixing a metastable SiO_2 colloidal crystalline array in a mixture of ethylene glycol (EG) and poly(ethylene glycol) methacrylate through photopolymerization. A high volume fraction of EG (46%) is introduced to the photonic gel before particle assembly, but not by swelling after polymerization, which leads to a more deformable composite than most reported opal gels. Compared to the traditional mechanochromic opal gel, this material is more sensitive to external forces and a total reflection wavelength shift of 150 nm can be achieved through stretching or bending. At the same time, the material retains all the advantages of opal gels such as a fast (in the millisecond range), reversible response, and repeatable reflection wavelength and intensity in cycling and fatigue tests.

Ge et al.[67] prepared a composite film consisting of a thin layer of quasi-amorphous array of SiO_2 nanoparticles of 221, 258, and 306 nm, embedded in bulk elastomeric PDMS. Angle-independent color was reflected by the particle arrays due to their short-range ordering but lack of long-range periodicity. The film was highly transparent (>90% transmittance for visible wavelengths) in the initial state. Upon mechanical stretching, the transmittance was dramatically reduced to 30% and displayed angle-independent structural color at a strain >40%. The change of optical responses is attributed to an increase in diffuse light scattering and absorption resulting from the formation of microwrinkles and voids during stretching. The color could be tuned by varying the nanoparticle size.

Lee et al.[45] injected $Fe_3O_4@SiO_2$ core-shell nanoparticles in between transparent top and bottom electrodes and demonstrated electrically tunable display pixels exhibiting angle-independent structural colors across the visible region (Figure 10(a)). The $Fe_3O_4@SiO_2$ nanoparticles have a large electrophoretic mobility in organic solvents and high optical contrast. Due to their negative surface charge, the $Fe_3O_4@SiO_2$ nanoparticles localized on the positive electrode upon application of a bias voltage, and the resultant increase in the local concentration induced the color changes. When the bias voltage was

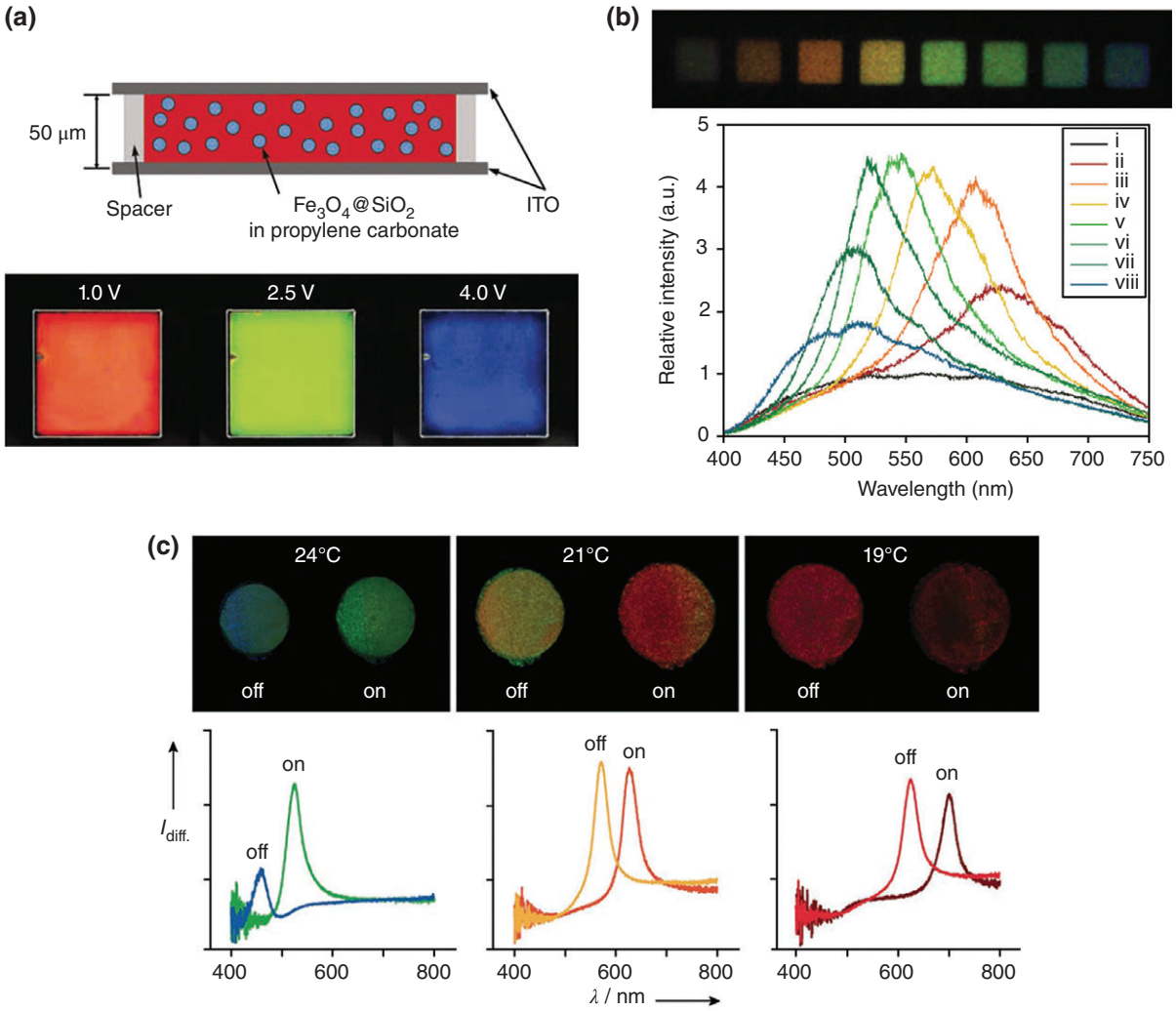

FIGURE 10 | (a) Tunability of a photonic display pixel as a function of applied electric potential difference.[45] (b) Generation of high-resolution multiple structural color patterns using M-Ink.[68] (c) Multicolor photochromic behavior of the porous gel. Photographs and reflection spectra of the porous poly(NIPA-co-AAB) gel in water at 19, 21, and 24°C before UV irradiation and after the equilibrium degree of swelling had been reached in response to the UV irradiation.[70]

increased from 1.0 V to 4.0 V, the photonic bandgap position shifted from 655 nm to 490 nm.

Kim et al.[68] developed a photonic crystal, termed M-Ink, the color of which was magnetically tunable and lithographically fixable. M-Ink consisted of a photocurable resin, solvation liquid, and superparamagnetic colloidal nanocrystal clusters comprising many single-domain magnetite nanocrystals capped with silica shells. Under an external magnetic field, the colloidal nanocrystal clusters were assembled to form chain-like structures along the magnetic field lines, balanced through the interaction of a magnetically induced attractive force and repulsive electrostatic and solvation forces. The color of light diffracted from the chain was determined by the interparticle distance within the chain (Figure 10(b)). Once the desired color was obtained from M-Ink by application of an external magnetic field, it could be fixed by solidifying the photocurable resin through UV exposure.

Walish et al.[69] demonstrated an electrically controlled, full-color tunable photonic crystal pixel in a simple lamellae-forming diblock copolymer. A hydrophilic/hydrophobic block copolymer, polystyrene-b-poly(2-vinylphyridine) (PS-P2VP), was spin-coated on the negative electrode of a pixel filled with an electrolytic fluid, 2,2,2-trifluoroethanol (TFE), where it formed a 1D photonic crystal. When the P2VP was swollen by the TFE, the polymer reflected red light. By applying a voltage to the substrate, the polymer film turned from red to green because of an electrochemical

reaction that produced trifluoroethoxide ions (TFX^-). TFX^- did not swell the P2VP as well as TFE did and thus the addition of TFX^- caused the P2VP domains to shrink, blueshifting the reflected light.

Tunable structural color can also be produced by photonic crystals made of organic molecules that change their geometry upon exposure to UV or visible light. Matsubara et al.[70] presented a porous gel capable of rapid light-triggered switching between two structural colors. The authors introduced a periodically ordered interconnecting porous structure and incorporated azobenzene units into the gel. Azobenzene derivatives are well-known photochromic compounds that exist in two different states, the *trans* form and the *cis* form, which can be interconverted reversibly by means of a light stimulus. Figure 10(c) shows the photoinduced change in the multi-structural color of the porous gel in water at different temperatures. Upon UV irradiation, a new spectral peak appeared at a longer wavelength than the corresponding peak observed in the dark at each temperature.

CONCLUSION

We have reviewed the structural colors displayed by various biological species. These structural colors originate from thin films, multilayers, photonic crystals, and isotropic structures. Some of the structural colors in animals are even tunable. These spectacular structural colors in biology have inspired a variety of artificially fabricated, multi-functional photonic structures and materials.[71] Iridescent structural colors have been produced by multilayers and different types of photonic crystals. By employing isotropic structures, non-iridescent structural colors have also been demonstrated. Some of the bio-inspired structural colors can be tuned by changing the lattice spacing and/or the optical constants of the materials by thermal, electrical, magnetic, optical, and other stimuli. Technologically, bio-inspired structural colors hold substantial promise for applications in sensing, security, display, cosmetics, decorations, paints, and many other areas.

REFERENCES

1. Vukusic P, Sambles JR, Lawrence CR, Wootton RJ. Quantified interference and diffraction in single Morpho butterfly scales. *Proc R Soc B Biol Sci* 1999, 266:1403. doi:10.1098/rspb.1999.0794.
2. Seago AE, Brady P, Vigneron J-P, Schultz TD. Gold bugs and beyond: a review of iridescence and structural colour mechanisms in beetles (Coleoptera). *J R Soc Interface* 2009, 6(Suppl 2):S165–S184. doi:10.1098/rsif.2008.0354.focus.
3. Vignolini S, Rudall PJ, Rowland AV, Reed A, Moyroud E, Faden RB, Baumberga JJ, Gloverc BJ, Steiner U. Pointillist structural color in Pollia fruit. *Proc Natl Acad Sci USA* 2012, 109:15712–15715. doi:10.1073/pnas.1210105109.
4. Lee HS, Shim TS, Hwang H, Yang SM, Kim SH. Colloidal photonic crystals toward structural color palettes for security materials. *Chem Mater* 2013, 25:2684–2690. doi:10.1021/cm4012603.
5. Choi SY, Mamak M, Von Freymann G, Chopra N, Ozin GA. Mesoporous bragg stack color tunable sensors. *Nano Lett* 2006, 6:2456–2461. doi:10.1021/nl061580m.
6. Hwang J, Song MH, Park B, Nishimura S, Toyooka T, Wu JW, Takanishi Y, Ishikawa K, Takezoe H. Electro-tunable optical diode based on photonic bandgap liquid-crystal heterojunctions. *Nat Mater* 2005, 4:383–387. doi:10.1038/nmat1377.
7. Vigneron JP, Simonis P. Natural photonic crystals. *Phys B Condens Matter* 2012, 407:4032–4036. doi:10.1016/j.physb.2011.12.130.
8. Ingram A, Parker A. A review of the diversity and evolution of photonic structures in butterflies, incorporating the work of John Huxley (The Natural History Museum, London from 1961 to 1990). *Philos Trans R Soc B Biol Sci* 2008, 363:2465–2480. doi:10.1098/rstb.2007.2258.
9. Sorger VJ, Zhang X. Physics. Spotlight on plasmon lasers. *Science* 2011, 333:709–710. doi:10.1126/science.1204862.
10. Yu K, Fan T, Lou S, Zhang D. Biomimetic optical materials: Integration of nature's design for manipulation of light. *Prog Mater Sci* 2013, 58:825–873. doi:10.1016/j.pmatsci.2013.03.003.
11. Xu J, Guo Z. Biomimetic photonic materials with tunable structural colors. *J Colloid Interface Sci* 2013, 406:1–17. doi:10.1016/j.jcis.2013.05.028.
12. Zhao Y, Xie Z, Gu H, Zhu C, Gu Z. Bio-inspired variable structural color materials. *Chem Soc Rev* 2012, 41:3297. doi:10.1039/c2cs15267c.
13. Saito A. Corrigendum: Material design and structural color inspired by biomimetic approach. *Sci Technol Adv Mater* 2012, 13:029501. doi:10.1088/1468-6996/12/6/064709.

14. Wang H, Zhang K-Q. Photonic crystal structures with tunable structure color as colorimetric sensors. *Sensors* 2013, 13:4192–4213. doi:10.3390/s130404192.
15. Karthaus O. *Biomimetics in Photonics*. London: CRC Press; 2012.
16. Yin Y. *Responsive Photonic Nanostructures*. London: The Royal Society of Chemistry; 2013. doi:10.1039/9781849737760.
17. Kinoshita S, Yoshioka S, Miyazaki J. Physics of structural colors. *Rep Prog Phys* 2008, 71:076401. doi:10.1088/0034-4885/71/7/076401.
18. John S. Strong localization of photons in certain disordered dielectric superlattices. *Phys Rev Lett* 1987, 53:2486–2489.
19. Yablonovitch E. Inhibited spontaneous emission in solid-state physics and electronics. *Phys Rev Lett* 1987, 58:2059–2062. doi:10.1103/PhysRevLett.58.2059.
20. Kinoshita S, Yoshioka S, Kawagoe K. Mechanisms of structural colour in the Morpho butterfly: cooperation of regularity and irregularity in an iridescent scale. *Proc Biol Sci* 2002, 269:1417–1421. doi:10.1098/rspb.2002.2019.
21. Okada N, Zhu D, Cai D, Cole JB, Kambe M, Kinoshita S. Rendering Morpho butterflies based on high accuracy nano-optical simulation. *J Opt* 2012, 42:25–36. doi:10.1007/s12596-012-0092-y.
22. Kinoshita S, Yoshioka S. Structural colors in nature: the role of regularity and irregularity in the structure. *ChemPhysChem* 2005, 6:1443–1459. doi:10.1002/cphc.200500007.
23. Zhu D, Kinoshita S, Cai D, Cole JB. Investigation of structural colors in Morpho butterflies using the nonstandard-finite-difference time-domain method: effects of alternately stacked shelves and ridge density. *Phys Rev Stat Nonlinear Soft Matter Phys* 2009, 80:51924. doi:10.1098/rspb.2002.2019.
24. Siddique RH, Diewald S, Leuthold J, Hölscher H. Theoretical and experimental analysis of the structural pattern responsible for the iridescence of Morpho butterflies. *Opt Express* 2013, 21:14351–14361. doi:10.1364/OE.21.014351.
25. Smith GS. Structural color of Morpho butterflies. *Am J Phys* 2009, 77:1010. doi:10.1119/1.3192768.
26. Kinoshita S, Yoshioka S, Fujii Y, Okamoto N. Photophysics of structural color in the Morpho butterflies. *Forma Tokyo* 2002, 17:103–121.
27. Welch VL, Vigneron JP. Beyond butterflies-the diversity of biological photonic crystals. *Opt Quantum Electron* 2007, 39:295–303. doi:10.1007/s11082-007-9094-4.
28. Parker AR, McKenzie DR. The cause of 50 million-year-old colour. *Proc Biol Sci* 2003, 270(Suppl): S151–S153. doi:10.1098/rsbl.2003.0055.
29. Bartl MH, Galusha JW, Richey LR, Gardner JS, Cha JN. Discovery of a diamond-based photonic crystal structure in beetle scales. *Phys Rev E Stat Nonlinear Soft Matter Phys*; 2012, 77:050904–050907. doi:10.1103/PhysRevE.77.050904.
30. Anderson TF, Richards AG. An electron microscope study of some structural colors of insects. *J Appl Phys* 1942, 13:748–758. doi:10.1063/1.1714827.
31. Gigantea EUCHROMa. Schillerfarben Von Euchroma Gigantea (L.): (Coleoptera: Buprestidae): Elektronenmikroskopische Untersuchung. *Elytra* 1972, 1:233–240.
32. Mitov M, Dessaud N. Depassement de la limite de reflexion de la lumiere des cristaux liquides cholesteriques: de Plusiotis resplendens aux gels a inversion d'helicite. *Comptes Rendus Chim* 2008, 11:253–260. doi:10.1016/j.crci.2007.03.020.
33. Michelson AA. On metallic colouring in birds and insects. *Philos Mag* 1911, 21:554–567. doi:10.1080/14786440408637061.
34. Caveney S. Cuticle reflectivity and optical activity in scarab beetles: the rôle of uric acid. *Proc R Soc Lond B Biol Sci* 1971, 178:205–225. doi:10.1098/rspb.1971.0062.
35. Yoshioka S, Kinoshita S. Effect of macroscopic structure in iridescent color of the peacock feathers. *Forma* 2002, 17:169–181.
36. Zi J, Yu X, Li Y, Hu X, Xu C, Wang X, Liu X, Fu R. Coloration strategies in peacock feathers. *Proc Natl Acad Sci USA* 2003, 100:12576–12578. doi:10.1073/pnas.2133313100.
37. Li Y, Lu Z, Yin H, Yu X, Liu X, Zi J. Structural origin of the brown color of barbules in male peacock tail feathers. *Phys Rev E Stat Nonlinear Soft Matter Phys* 2005, 72:1–4. doi:10.1103/PhysRevE.72.010902.
38. Osorio D, Ham AD. Spectral reflectance and directional properties of structural coloration in bird plumage. *J Exp Biol* 2002, 205:2017–2027.
39. Jun N. The iridescent colors of hummingbird feathers. *J Proc Am Philos Soc* 1960, 104:249–253.
40. Prum RO, Torres R, Williamson S, Dyck J. Two-dimensional Fourier analysis of the spongy medullary keratin of structurally coloured feather barbs. *Proc R Soc B Biol Sci* 1999, 266:13–22. doi:10.1098/rspb.1999.0598.
41. Stavenga DG, Tinbergen J, Leertouwer HL, Wilts BD. Kingfisher feathers - colouration by pigments, spongy nanostructures and thin films. *J Exp Biol* 2011, 214:3960–3967. doi:10.1242/jeb.062620.
42. Teyssier J, Saenko SV, van der Marel D, Milinkovitch MC. Photonic crystals cause active colour change in chameleons. *Nat Commun* 2015, 6:6368. doi:10.1038/ncomms7368.

43. Saenko SV, Teyssier J, van der Marel D, Milinkovitch MC. Precise colocalization of interacting structural and pigmentary elements generates extensive color pattern variation in Phelsuma lizards. *BMC Biol* 2013, 11:105. doi:10.1186/1741-7007-11-105.
44. Gur D, Palmer BA, Leshem B, Oron D, Fratzl P, Weiner S, Addadi L. The mechanism of color change in the neon tetra fish: a light-induced tunable photonic crystal array. *Angew Chem Int Ed* 2015, 54:12426–12430. doi:10.1002/anie.201502268.
45. Lee I, Kim D, Kal J, Baek H, Kwak D, Go D, et al. Quasi-amorphous colloidal structures for electrically tunable full-color photonic pixels with angle-independency. *Adv Mater* 2010, 22:4973–4977. doi:10.1002/adma.201001954.
46. Okubo T. In: Kinoshita S, Yoshioka S, eds. *Structural Colors in Biological Systems. Princples and Applications*. Osaka: Osaka University Press; 2005, 267.
47. Potyrailo RA, Bonam RK, Hartley JG, Starkey TA, Vukusic P, Vasudev M, Bunning T, Naik RR, Tang Z, Palacios MA, et al. Towards outperforming conventional sensor arrays with fabricated individual photonic vapour sensors inspired by Morpho butterflies. *Nat Commun* 2015, 6:7959. doi:10.1038/ncomms8959.
48. Huang J, Wang X, Wang ZL. Controlled replication of butterfly wings for achieving tunable photonic properties. *Nano Lett* 2006, 6:2325–2331. doi:10.1021/nl061851t.
49. Watanabe K, Hoshino T, Kanda K, Haruyama Y, Matsui S. Brilliant blue observation from a Morpho-butterfly-scale quasi-structure. *Japanese J Appl Phys Part 2 Lett* 2005, 44:1–4. doi:10.1143/JJAP.44.L48.
50. Watanabe K, Hoshino T, Kanda K, Haruyama Y, Kaito T, Matsui S. Optical measurement and fabrication from a Morpho-butterfly-scale quasistructure by focused ion beam chemical vapor deposition. *J Vac Sci Technol B Microelectron Nanom Struct* 2005, 23:570. doi:10.1116/1.1868697.
51. Aryal M, Ko D-H, Tumbleston JR, Gadisa A, Samulski ET, Lopez R. Large area nanofabrication of butterfly wing's three dimensional ultrastructures. *J Vac Sci Technol B Microelectron Nanom Struct* 2012, 30:061802. doi:10.1116/1.4759461.
52. Wu Z, Lee D, Rubner MF, Cohen RE. Structural color in porous, superhydrophilic, and self-cleaning SiO_2/TiO_2 Bragg stacks. *Small* 2007, 3:1445–1451. doi:10.1002/smll.200700084.
53. Yoon J, Lee W, Thomas EL. Optically pumped surface-emitting lasing using self-assembled block-copolymer-distributed bragg reflectors. *Nano Lett* 2006, 6:2211–2214. doi:10.1021/nl061490h.
54. Davis KE, Russel WB, Glantschnig WJ. Settling suspensions of colloidal silica: observations and X-ray measurements. *J Chem Soc Faraday Trans* 1991, 87:411. doi:10.1039/ft9918700411.
55. Jiang P, Bertone J. Single-crystal colloidal multilayers of controlled thickness. *Chem Mater* 1999, 11:2132–2140. doi:10.1021/cm990080+.
56. Gu ZZ, Fujishima A, Sato O. Fabrication of high-quality opal films with controllable thickness. *Chem Mater* 2002, 14:760–765. doi:10.1021/cm0108435.
57. Prevo BG, Velev OD. Controlled, rapid deposition of structured coatings from micro- and nanoparticle suspensions. *Langmuir* 2004, 20:2099–2107. doi:10.1021/la035295j.
58. Forster JD, Noh H, Liew SF, Saranathan V, Schreck CF, Yang L, Park JG, Prum RO, Mochrie SG, O'Hern CS, et al. Biomimetic isotropic nanostructures for structural coloration. *Adv Mater* 2010, 22:2939. doi:10.1002/adma.200903693.
59. Zhang Y, Dong B, Chen A, Liu X, Shi L, Zi J. Using cuttlefish ink as an additive to produce non-iridescent structural colors of high color visibility. *Adv Mater* 2015, 27:4719–4724. doi:10.1002/adma.201501936.
60. Chung K, Yu S, Heo CJ, Shim JW, Yang SM, Han MG, Lee HS, Jin Y, Lee SY, Park N, et al. Flexible, angle-independent, structural color reflectors inspired by morpho butterfly wings. *Adv Mater* 2012, 24:2375–2379. doi:10.1002/adma.201200521.
61. Ballato J, James A. A ceramic photonic crystal temperature sensor. *J Am Ceram Soc* 2004, 82:2273–2275. doi:10.1111/j.1151-2916.1999.tb02078.x.
62. Yoshino K, Shimoda Y, Kawagishi Y, Nakayama K, Ozaki M. Temperature tuning of the stop band in transmission spectra of liquid-crystal infiltrated synthetic opal as tunable photonic crystal. *Appl Phys Lett* 1999, 75:932. doi:10.1063/1.124558.
63. Kubo S, Gu Z-Z, Takahashi K, Ohko Y, Sato O, Fujishima A. Control of the optical band structure of liquid crystal infiltrated inverse opal by a photoinduced nematic-isotropic phase transition. *J Am Chem Soc* 2002, 124:10950–10951. doi:10.1021/ja026482r.
64. Fudouzi H, Xia Y. Colloidal crystals with tunable colors and their use as photonic papers. *Langmuir* 2003, 19:9653–9660. doi:10.1021/la034918q.
65. Fudouzi H, Sawada T. Photonic rubber sheets with tunable color by elastic deformation. *Langmuir* 2006, 22:1365–1368. doi:10.1021/la0521037.
66. Yang D, Ye S, Ge J. From metastable colloidal crystalline arrays to fast responsive mechanochromic photonic gels: an organic gel for deformation-based display panels. *Adv Funct Mater* 2014, 24:3197–3205. doi:10.1002/adfm.201303555.
67. Ge D, Lee E, Yang L, Cho Y, Li M, Gianola DS, Yang S. A robust smart window: reversibly switching from high transparency to angle-independent

structural color display. *Adv Mater* 2015, 27:2489–2495. doi:10.1002/adma.201500281.

68. Kim H, Ge J, Kim J, Choi S, Lee H, Lee H, Park W, Yin Y, Kwon S. Structural colour printing using a magnetically tunable and lithographically fixable photonic crystal. *Nat Photonics* 2009, 3:534–540. doi:10.1038/nphoton.2009.141.
69. Walish JJ, Kang Y, Mickiewicz RA, Thomas EL. Tunable full-color pixels: bioinspired electrochemically tunable block copolymer full color pixels. *Adv Mater* 2009, 21:1–4. doi:10.1002/adma.200990117.
70. Matsubara K, Watanabe M, Takeoka Y. A thermally adjustable multicolor photochromic hydrogel. *Angew Chem Int Ed* 2007, 46:1688–1692. doi:10.1002/anie.200603554.
71. Greanya V. *Bioinspired in Photonics: Optical Structures and Systems Inspired by Nature*. Florida: CRC Press; 2015.